ACS chemical biology

Articles

pubs.acs.org/acschemicalbiology

Tracing Fatty Acid Metabolism by Click Chemistry

Christoph Thiele,*[,†] Cyrus Papan,[‡] Dominik Hoelper,[†] Kalina Kusserow,[†] Anne Gaebler,[†] Mario Schoene,[†] Kira Piotrowitz,[†] Daniel Lohmann,[†] Johanna Spandl,[†] Ana Stevanovic,[†] Andrej Shevchenko,[‡] and Lars Kuerschner[†]

[†]LIMES Life and Medical Sciences Institute, University of Bonn, Carl-Troll-Strasse 31, D-53115 Bonn, Germany

[‡]Max Planck Institute of Molecular Cell Biology and Genetics, Pfotenhauerstrasse 108, D-01307 Dresden, Germany

Supporting Information

ABSTRACT: Fatty acids are abundant constituents of all biological systems, and their metabolism is important for normal function at all levels of an organism. Aberrations in fatty acid metabolism are associated with pathological states and have become a focus of current research, particularly due to the interest in metabolic overload diseases. Here we present a click-chemistry-based method that allows tracing of fatty acid metabolism in virtually any biological system. It combines high sensitivity with excellent linearity and fast sample turnover. Since it is free of radioactivity, it can be combined with any other modern analysis technology and can be used in high-throughput applications. Using the new method, we provide for the first time an analysis of cellular fatty metabolism with high time resolution and a comprehensive comparison of utilization of a broad spectrum of fatty acids in hepatoma and adipose cell lines.

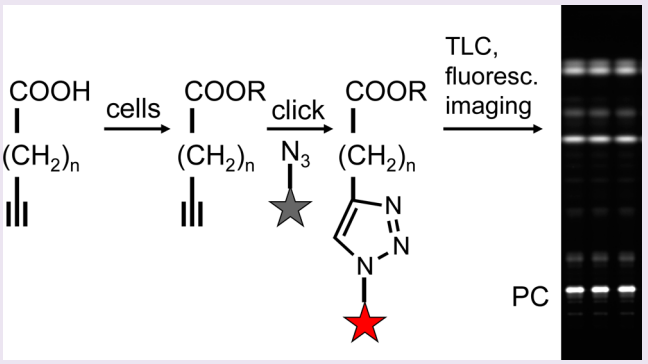

The study of metabolic overload diseases has become an important focus of biomedical research, driven by the need to understand the consequences of overcaloric westernized diet. Since metabolic overload usually leads to obesity, studies of fatty acid metabolism are a central aspect of current metabolism research. For that, detailed quantitative information about fatty acid metabolism from all available model systems, such as purified proteins, cultivated cell lines, primary cells, isolated organs, and whole organisms, is needed. While the need for these data is steadily increasing, we face a concomitant decrease of the accessibility and acceptance of the major technology used to obtain these data in the past 60 years,[1] *i.e.*, radioisotope tracing. Handling radioisotopes requires special laboratories and official permissions and causes major costs for both purchase of substances and disposal of radioactive waste. Furthermore, many researchers are reluctant to use radiolabeled compounds because of safety concerns or other reasons. Also, these methods suffer from limited sensitivity because the relevant isotopes for fatty acid tracing, ^{3}H and ^{14}C, have moderate or low specific activities and require long exposure times in order to obtain a meaningful result.

Click chemistry allows the sensitive and specific detection of compounds containing azido groups or terminal alkynes,[2] which can be integrated into fatty acids without major disturbance of the structure of the hydrophobic hydrocarbon chains. Other click-labeled precursors are already in use to replace radioactive molecules in metabolic labeling experiments, including amino acids,[3,4] carbohydrates,[5] nucleotides,[6] or lipids.[7] Click-labeled fatty acids so far were used to monitor protein lipidation.[8−10] Their application to follow lipid metabolism has been hampered so far by the lack of protocols that allow sensitive and quantitative detection of click-labeled lipid metabolites. The present paper solves this problem by the use of a highly optimized protocol for fluorogenic click reaction with subsequent TLC separation and fluorescence detection.

RESULTS AND DISCUSSION

Method Design and Evaluation. Cells contain numerous different fatty acids with different numbers of carbon atoms and double bonds. Previous studies have described clickable azido- and alkyne-analogues with various chain lengths of saturated fatty acids, recently reviewed in ref 7, and alkyne-linoleate and -arachidonate,[11] but no clickable derivative of oleate. For radioisotope tracing of fatty acid metabolism, oleate and palmitate are most frequently used, because they represent the most abundant fatty acids in mammalian circulation and in cellular lipids. We synthesized analogues of oleate and various saturated fatty acids containing terminal alkyne groups for click detection (see Supplementary Figure 1 and Supporting Information). These fatty acids were supplemented into normal growth or perfusion media for 2−120 min, followed by

Received: August 7, 2012
Accepted: September 21, 2012
Published: September 21, 2012

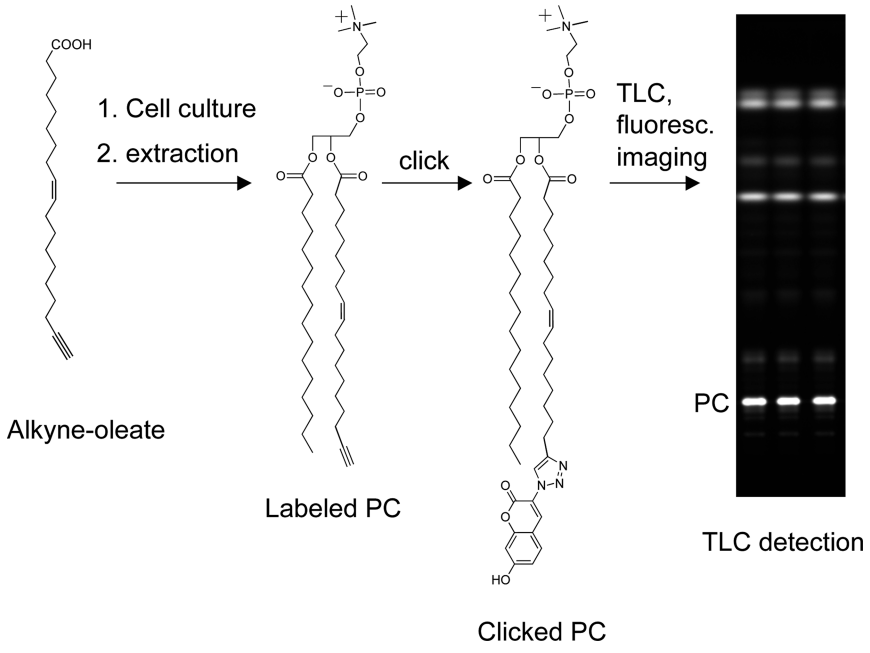

Figure 1. Schematic representation of a typical workflow of the method. Alkyne lipid precursors are supplemented to cell culture where they become incorporated into cellular lipids. These are extracted and reacted with the fluorogenic dye 3-azido-7-hydroxycoumarin in the presence of copper(I). The fluorescent lipids are then separated on TLC plates and detected by fluorescence imaging.

collection of the biological material and standard lipid extraction.

Extracts were reacted with 3-azido-7-hydroxycoumarin,[12] a small, nonpolar dye, which does not dominate the migration behavior of the reaction products in subsequent TLC separation. In addition, 3-azido-7-hydroxycoumarin is non-fluorescent and forms a fluorescent triazolyl-coumarin derivative only upon click reaction with the alkyne fatty acid[12] (Figure 1), avoiding the problem of strong background signal from excess of unreacted dye. The click reaction was optimized to detect the very small amounts of labeled lipids that are obtained in a typical labeling experiment. Systematic optimization of volumes, concentrations, temperature, reaction time, solvents, and source of Cu(I) lead to a virtually complete reaction for analyte concentrations up to 15 μM (Supplementary Figure 2a). The importance of the dye concentration is illustrated in Supplementary Figure 2b. Dye concentrations exceeding 60 μM did not lead to stronger signal but only to increased background.

After the click reaction, products were separated on standard silica gel TLC plates, using a separation system with two solvents of different polarity. The clicked lipids behaved very similarly to their natural counterparts, *i.e.*, the normal order of mobility is unchanged (Supplementary Figure 2b, also compare Supplementary Figure 3).

To ensure that all coumarin dye molecules on the TLC plate are in the more strongly fluorescent deprotonated phenolate form,[13] the dried plate was soaked for few seconds in a solution of *N*,*N*-diisopropylethylamine (Hünigs base), a volatile non-fluorescent basic reagent, in hexane, resulting in a striking 60-fold increase of the signal (Supplementary Figure 2b,c).

Sensitivity and linear dynamic range of the assay were determined using the cholesterol ester of alkyne-oleate as a model substance. With a reaction volume of 30 μL, the lower detection level was at a concentration of 13.5 nM corresponding to 0.4 pmol total substance (Figure 2a). Over

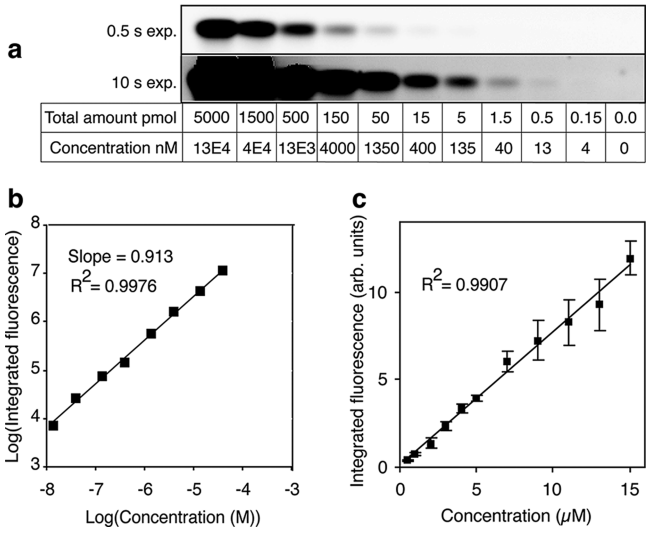

Figure 2. Sensitivity and linearity. The cholesterol ester of alkyne-oleate at the indicated concentrations was subjected to detection reaction, TLC separation, and fluorescence imaging using the standard protocol. (a) Images of the same plate exposed for 0.5 or 10 s. (b) Quantification of the integrated fluorescence of panel a. Data are displayed in a double log plot. The slope of 0.91 indicates only small deviations from linearity over a concentration range of 3.5 magnitudes. Note that the sample with the highest concentration in panel a was not included in the analysis, because the analyte concentration exceeded the dye concentration. (c) The same experiment was performed with samples at the practically most relevant concentration range of 0.5−15 μM. These data are displayed in a nonlogarithmic plot as mean ± SD of three independent experiments.

a concentration range from 13.5 nM to 40 μM, the response curve was nearly linear, as shown by the slope of 0.91 in a double logarithmic plot (Figure 2b). A similar experiment with more data points in a more narrow range showed linearity over

dx.doi.org/10.1021/cb300414v | *ACS Chem. Biol.* 2012, 7, 2004−2011

the practically most important concentration range between 0.5 and 15 μM (Figure 2c).

To identify labeled spots using co-migrating lipid standards, we synthesized TAG, 1,2-DAG, 1,3-DAG, 1-MAG, CE, PE, PA, and PC, all bearing alkyne-oleate. Supplementary Figure S3 shows the purity of the standards and also demonstrates the good separation in the two-solvent TLC system.

In order to evaluate the usefulness of alkyne-fatty acids as tracers for natural fatty acids, we compared the metabolism of alkyne-oleate and natural oleate. For that, we incubated freshly isolated hepatocytes with equal concentration of alkyne-oleate and oleate plus a tracer amount of ^{3}H-oleate. After 10 min of labeling and a 20 min chase, lipids were extracted, split into equal aliquots, and analyzed either by the standard click procedure or by TLC followed by fluorography (Figure 3a).

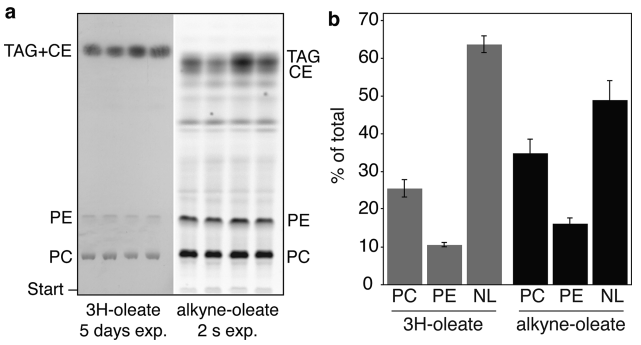

Figure 3. Comparison between ^{3}H-oleate and alkyne-oleate labeling. Freshly isolated mouse hepatocytes were plated on 10 cm dishes in Williams E medium plus 1% FA-free BSA and labeled at 37 °C for 10 min with a mixture of 20 μM alkyne-oleate, 20 μM oleate, and 3 μCi/mL of ^{3}H-oleate. After a 20 min chase in Williams E medium +1% FA-free BSA, cells were washed and scraped, and lipids were extracted. Equal aliquots (one-fourth of total) were either directly applied on TLC, sprayed with scintillant, and exposed to X-ray film (panel a, left), or subjected to click reaction, TLC, and imaging following the standard protocol (panel a, right). Signals were quantified either by scraping, extraction, and scintillation counting (panel b, ^{3}H-oleate) or by integration of signals from the fluorescence image (panel b, alkyne-oleate). All differences between bars are statistically significant with $p < 0.01$ (one-way ANOVA). NL: neutral lipids, TAG + CE.

Qualitatively both methods gave the same results, with most of the label found in PC, PE, and neutral lipids (NL). Despite a 5-day exposure, the fluorography showed clearly visible bands only for the three most abundant products. In contrast, a 2 s exposure of the clicked lipids revealed a clear picture with much stronger signal and less background, showing several additional weak bands of minor metabolites. For a quantitative evaluation, the click image was directly quantified, while radioactive bands were scraped, and lipids were extracted and subjected to scintillation counting. Comparing the three major products, the amount of label in neutral lipids was slightly smaller for alkyne-oleated (49%) than for ^{3}H-oleate (64%); the difference was proportionally distributed over PC and PE. For a closer inspection of the distribution of labeled species, we analyzed labeled lipids by mass spectrometry and extended the analysis to alkyne-palmitate. This analysis is described in detail in Supplementary Figures 4 and 5 and Supporting Information. Hepatocytes were labeled with alkyne-oleate and -palmitate for three different labeling times, and lipids were extracted and analyzed by click labeling or mass spectrometry. Patterns of labeled lipid classes showed characteristic differences between the two fatty acids, with alkyne-oleate having a stronger preference for incorporation into TAG, whereas alkyne-palmitate showed preference for labeling of PC, indicating that the alkyne fatty acids retain characteristic properties of the unlabeled natural compounds. Detailed mass spectrometrical analysis first showed that the applied alkyne fatty acids did not influence the species composition of cellular phospholipids. Also, when combined with other fatty acids in PC species, alkyne-palmitate and alkyne-oleate showed the same characteristic preferences for certain combinations as did their respective natural counterparts. These results indicate that alkyne fatty acids of different chain length and saturation are valid models for the respective natural compounds, which was confirmed by metabolic studies with a broader selection of labeled compounds (see application examples in Figures 5 and 6 and Supplementary Figure 7)

Advantages. The sensitivity of click-labeling is higher than that of a ^{14}C-labeling experiment and at least comparable to that of a ^{3}H-labeling experiment. The lower limit of detection of 0.4 pmol corresponds to 24 pCi of ^{14}C-fatty acid or 20 nCi of ^{3}H-fatty acid. While the former would normally not be detectable on an X-ray film,[14] the latter would require overnight exposure on X-ray film for reliable detection, compared to about a second for the fluorescence imaging. The linear signal generated by the click procedure allows direct quantification. Analysis of a TLC plate with 12 lanes and 10 bands per lane can be performed in less than 1 h and can be automated using appropriate software macros. The method is highly versatile and can be adapted to virtually any experimental condition or model organism. Here, the lack of radioactivity is particularly beneficial, because it avoids the restrictions that are frequently faced if a complex experimental setup needs to be combined with radioactive work, allowing spontaneous barrier-free experiments. Regarding cost efficiency, click labeling requires investment into a camera/illumination unit (which frequently is present in laboratories anyway and can be adapted at low costs) and some chemicals but saves the costs and space for isotope lab, liquid scintillation counting, X-ray films and a film developer, for purchase and disposal of radioactivity, and for special medical surveillance of personal. The same argument holds true when click labeling is compared to mass spectrometry (see below), which requires large investments into LC−MS mass spectrometers, maintenance, and well-trained staff. Furthermore, the higher sensitivity allows downscaling of experiments with the concomitant reduction of costs for cell culture media and growth supplements. Regarding time and productivity, a complete click labeling experiment including the quantitative analysis and evaluation is normally finished in one working day. In contrast, the radioactive method needs more time already in the experiment itself because of the typical safety precautions. Once the actual experiment is done, it takes typically 2−6 days for the exposure of the TLC plate, and another day for the scraping/extraction/scintillation counting procedure.

Limitations. Like the corresponding radiolabeling procedure, our method cannot give lipid species resolution. If this is needed, fluorescent analysis should be complemented by mass spectrometrical analysis as demonstrated in Supplementary Figures S4 and S5, where the alkyne-oleate or -palmitate are registered as unique fatty acids C19:3 or C17:2, respectively. Corresponding clicked products are also identifiable in direct shotgun mass spectrometric analysis *via* data-dependent acquisition of MS/MS spectra and *boolean* scans.[15] Future

developments in stable isotope mass spectrometric tracing[16] could allow pulse-chase fatty acid tracing with similar sensitivities as presented here. This would offer the perspective of complementing the specific advantages of the click-labeling system, *i.e.*, rapid parallel sample processing and quantification of all lipid classes independent of internal standards, with the perfect species resolution and the use of a natural tracer offered by mass spectrometry. For click labeling, the lipid class resolution depends on the TLC system used. The system applied in this study is optimized for rather short (2−30 min) pulse/chase studies, where PC, PA, PE, DAG, TAG, and CE are dominant. If necessary, other TLC systems[17] or HPLC separation with online fluorescence detection can be applied. Other limitations are inherent to the use of the alkyne fatty acids. They resemble their natural counterparts in many aspects but are not identical to them and may show subtle differences as shown for example in Figure 3. Two other limitations affect special aspects of metabolism: If ^{3}H-fatty acids are used, β-oxidation can be followed by the release of tritiated water. Alkyne fatty acids can be substrates of mitochondrial β-oxidation,[18] but since the terminal triple bond is unstable after degradation to propiolic acid,[19] we cannot follow a product indicative of the β-oxidation. The other aspect is inhibition of fatty acid ω-hydroxylases[20] and some prostaglandin hydroxylases[21] by terminal alkyne fatty acids. In cellular systems, in which ongoing ω-hydroxylation has a major function, *e.g.*, keratinocytes, alkyne fatty acids should be used with caution and preferably for short labeling periods.

Apart from the applications shown below, the method opens numerous perspectives of future experiments. Evidently, its application is not confined to the feeding of fatty acids but will include the use of labeled sphingolipids and sterols, as well as the use of alkyne fatty acyl-CoA and other alkyne lipids to monitor acyl-transferases or other lipid-metabolizing enzymes *in vitro*. Finally, combination with light microscopic imaging is a genuine possibility for alkyne-lipids,[22−24] not available for radiolabeled compounds. In preliminary experiments, we were able to image our alkyne-fatty acids after incorporation into cellular lipids by click reaction with various fluorescent dyes. This will need careful evaluation, because one would expect accessibility problems of the labeled long chain fatty acids in the core of the lipid bilayer. Nonetheless, the combination of the two methods has potential for studies of spatial organization of metabolism.

Applications. To explore application in basic model systems, *E. coli* bacteria were incubated in minimal medium with either of the two alkyne fatty acids, giving incorporation into PE and PG (Figure 4, lanes 1 and 2) at a ratio of 78/22 for alkyne-oleate and 85/15 for alkyne-palmitate, consistent with previous determinations of *E. coli* phospholipid class distribution.[25] Incorporation of alkyne-oleate into *Saccharomyces cerevisiae*, one of the classical model systems of lipidology, resulted in strong labeling of phospholipids and TAG (Figure 4, lane 5).

Drosophila melanogaster is a powerful genetic model system with increasing importance for lipid research. To demonstrate fatty acid metabolism in *Drosophila* tissues, we opened the cuticle of single L3 larvae and incubated them for 30 min in the respective alkyne fatty acid solution. Lanes 3 and 4 of Figure 4 demonstrate incorporation into PC, PE, and TAGs. There was a large difference between metabolism of the two alkyne fatty acids: while similar amounts of both fatty acids were found in PC, large amounts of alkyne-oleate but much less alkyne-palmitate was incorporated into PE. This reflects both the total phospholipids class distribution and the fatty acid composition of *Drosophila* membrane lipids.[26]

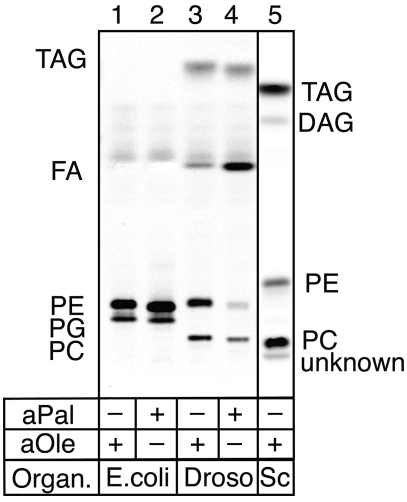

Figure 4. Application in different model systems. *E. coli* (E. coli) was grown for 3 h with 20 μM alkyne fatty acids as indicated, single *Drosophila* L3 larvae (Droso) were opened and incubated for 30 min with 50 μM alkyne lipids as indicated. *Saccharomyces cerevisiae* (Sc) was incubated for 2 h with 50 μM alkyne-oleate. Lipids were extracted and lipid extracts were subjected to detection reaction, TLC separation and fluorescence imaging using the standard protocol. The amounts loaded correspond to 1 mL *E. coli* culture (lanes 1, 2), one single L3 larva (lanes 3, 4) and 2 mL of yeast culture (lane 5). Note that lanes 1−4 are from one plate, lane 5 is from a separate experiment with different running distances of solvent systems 1 and 2, leading to different positions of lipids on the plate.

Kinetic pulse-chase analysis of fatty acid metabolism is an interesting application because it allows obtaining detailed quantitative data of anabolic lipid flux. COS7 cells were pulse-labeled for 2 min with alkyne-oleate followed by chases between 1 and 30 min (Figure 5a) leading to incorporation of fatty acid into various lipids (TAG, DAG, PE, PA, PC, and an unidentified lipid XY, presumably PI or PS). Quantification in Figure 5b gave a detailed kinetic picture of fatty acid metabolism in living cells. The first detectable metabolite, PA, rapidly decayed with a half live of 2 min to form DAG, which decayed with a half-life of about 5 min to form mostly PC, which increased from initially 28% to 63% of total labeled lipid. In contrast, PE and the phospholipid XY showed nearly constant labeling over the entire experiment. Under these experimental conditions (growth of cells in lipid-depleted media before the pulse labeling), TAG is a rather minor component, increasing from initially 5% to 10% after 30 min. The kinetic profiles of PA, DAG, and PC beautifully demonstrate the flow of fatty acid along the Kennedy pathway of PC biosynthesis (Figure 5c, black arrows). To our knowledge, this is the first time that the rapid initial steps of the Kennedy pathway, particularly the PA to DAG conversion, have been traced in living cells. Note that the PC curve does not start at 0%, as would be expected if the Kennedy pathway were the only route to incorporate fatty acids into PC. Instead, there is an offset that can be explained by the contribution of direct incorporation of labeled fatty acid during the pulse period to form PC from lyso-PC by LPCAT, which is part of the Lands cycle (Figure 5c, red arrows). The data therefore allow direct determination of relative contributions of the two

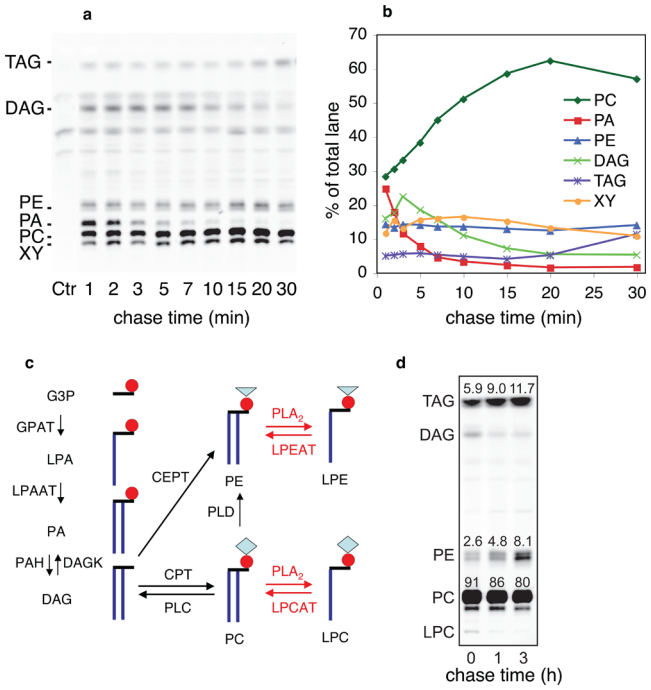

Figure 5. Applications in pulse-chase analysis and model systems. (a, b) Pulse chase alkyne-oleate labeling of COS7 cells. Cells grown overnight in DMEM + 10% (v/v) DL-FCS were pulse labeled for 2 min with 50 μM alkyne-oleate in Ringer buffer plus 1% FA-free BSA. Pulse medium was removed, and cells were washed with PBS/1% (w/v) FA-free BSA and chased in DMEM + 10% (v/v) DL-FCS + 50 μM oleate for times as indicated. Chase media were removed, and cells were washed with ice-cold PBS/1% (w/v) FA-free BSA and PBS and collected. Lipids were extracted and analyzed according to the standard procedure. (b) Quantification of panel a. Data are expressed as % of total signal per lane. Bands were identified by co-migrating synthetic standards. XY denotes an unidentified (phospho)lipid, likely PS or PI, for which we have not yet synthesized an according standard. (c) Pathways of fatty acid incorporation. Black arrows: Kennedy-pathway. Red arrows: Lands-cycle. (d) COS7 cells were incubated for 1 h with 20 μM of *sn*-1-alkyne-oleoyl-*sn*-2-lysoPC (prepared from dialkyne-oleoyl-PC by snake venom PLA2 digestion and purification on a silica column). The labeling medium was removed, and cells cwere hased for 1 or 3 h, followed by lipid extraction and click detection using the standard protocol. The picture shows an exposure with a saturated PC band to better visualize the PE and TAG; the quantification was done from a non-saturated exposure. Numbers in the picture indicate the fraction of PC, PE, and TAG as % of lane. Note that the supplemented LPC is rapidly converted to PC followed by slow conversion to PE and TAG, presumably by PLD- and PLC-dependent pathways.

pathways. For PE, the labeling *via* the Lands cycle appears to be dominant over the Kennedy pathway, since the labeling apparently did not increase during the 30 min chase period. To analyze whether over longer periods some of the initially formed PC is further metabolized to other glycerolipids, we performed long-term labeling with *sn*-1-alkyne-oleoyl-*sn*-2-lysoPC, which resulted, as expected,[27] in very strong labeling of cellular PC (Figure 5d, left lane). Upon 1 or 3 h chase (Figure 5d, mid and right lane), increasing fractions of the label were found in PE and TAG, consistent with metabolism mediated by PLD- or PLC-dependent pathways.

Finally, we analyzed the differential metabolism of fatty acids by adipocytes and hepatoma cells. Driven by the use of medium chain triglycerides as diet components for body weight reduction or in parenteral nutrition,[28] there are numerous studies in hepatocytes and adipocytes comparing metabolism of labeled palmitate or oleate with labeled octanoate,[28−31] but a comprehensive analysis covering metabolism of a broad spectrum of labeled fatty acids in different cell types has not been presented to date. Therefore, a broad range of terminal alkyne fatty acids (C5−C19) were fed to differentiated 3T3-L1 adipocytes and to HuH7 hepatoma cells at 50 μM for 1 h. Lipid extracts were either directly click-analyzed (Figure 6a,b) or subjected to alkaline hydrolysis followed by click-analysis (panels c,d). The hepatoma cells did not incorporate significant amounts of short and medium chain precursors (C5−C11) into phospholipids or neutral lipid (panel b), while C13, C17, and C19 fatty acids were used for synthesis of both phospholipids and neutral lipids. Alkaline hydrolysis (panel d) showed no detectable elongation or shortening of the incorporated fatty acids. In striking difference, 3T3-L1 adipocytes incorporated significant amounts of all fatty acids longer than six C-atoms (panel a). Combination of quantitative analysis of incorporation into lipid classes (panel e) and fatty acid length determination after alkaline hydrolysis (panel c) revealed the complexity of fatty acid usage in these cells. The C7 and C9 fatty acids were partially elongated to C17, and the C9 fatty acid was also partially shortened to C7. The C7 and C9 fatty acids were predominantly found in TAG (see the low mobility TAG in lanes 3 and 4), while the elongated species were incorporated into DAG and phospholipids (see the PC band in lanes 3 and 4, which have a higher mobility than the PC band in lane 5 and equal that of PC in lane 7). Part of the elongated fatty acid was also found in TAG (see the high mobility TAG bands labeled with an asterisk in lanes 3 and 4). Fatty acids C11, 13, 17, and 19 were neither elongated nor shortened during the 60 min time period of feeding but were incorporated directly (panel c). Quantitatively, the C11 and C13 fatty acids were predominantly found in TAG, while C17 and C19 equally distributed over phospholipids and neutral lipids. Also, major amounts of C11 and C13 fatty acids were found in the intermediate DAG. Globally, this analysis demonstrates that fatty acid metabolism very specifically depends on cell type and fatty acid chain length. It shows that it is not sufficient to study two or three different fatty acids, because each single fatty acid has an individual metabolic profile governed by the relative rates of uptake, elongation, degradation, and the various possible acylation reactions. A striking example is the C11 alkyne fatty acid. In hepatoma cells, it is not used at all in anabolism; in 3T3-L1 cells it is found in TAG and DAG, but only in traces in phospholipids. It appears that it can be used preferentially by DGAT enzymes to acylate DAG and also to some extent by GPAT and/or LPAAT resulting in the labeled DAG. This DAG appears to be a poor substrate for pathways leading to phospholipids, because hardly any phospholipid is found despite a major pool of labeled DAG. The C7 alkyne fatty acid is another interesting example for differential use in acylation reactions. Whereas about 80% of the labeled DAG contains elongated species, only 16% of the labeled TAG is elongated, while the majority contains the C7 acid, indicating that the major pathway for its use is by DGAT, but not by GPAT and LPAAT. Studies like this should become part of a routine metabolic characterization of cells and tissues. An even broader coverage of labeled fatty acids, including very long and polyunsaturated alkyne species,[11] will further increase the value of the findings.

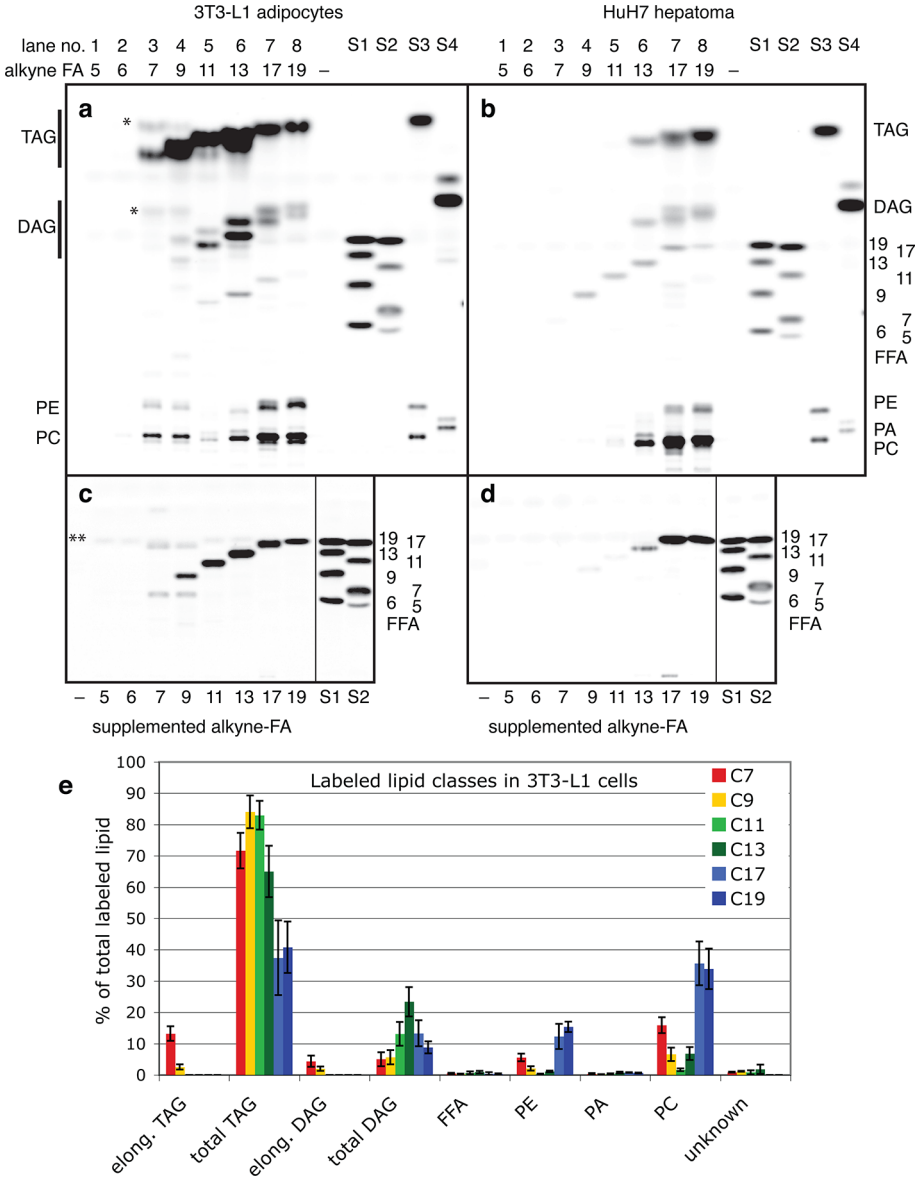

Figure 6. Cell type and chain length specific fatty acid metabolism. 3T3-L1 adipocytes (a, c) or HuH7 hepatoma cells (b, d) were grown in 3.5 or 6 cm plates, respectively, and supplemented for 1 h with 50 μM of ω-alkyne fatty acids as indicated below the figure (numbers in the labeling refer to total number of C-atoms including the triple bond; 5−17 are saturated (except for the ω-alkyne group) FAs, 19 is alkyne oleate). Cells were washed, scraped, and subjected to lipid extraction, and lipids extracts were dried. One-quarter of the extract was subjected to detection reaction, TLC separation, and fluorescence imaging using the standard protocol (panels a, b). A second quarter was subjected to alkaline hydrolysis followed by detection reaction, TLC separation, and fluorescence imaging (panels c, d). Lanes S1−S4 are clicked synthetic standards as indicated at the right of panel b. Note that standards S3 + S4 are synthesized using alkyne-oleate (C19) and therefore have higher mobility than the corresponding species with shorter fatty acids in lanes 3−7. The asterisks in panel a indicate the elongated TAG and DAG species, and the double asterisk in panel c indicates a background band. (e) Quantification of data in panel a. The bars correspond to mean ± SD of three independent experiments.

METHODS

Synthesis. Chemical synthesis of alkyne-lipids used in this study can be found in Supporting Information.

Cell Culture. A431 and COS7 cells were maintained in DMEM (Gibco 31966), supplemented with 10% (v/v) FCS. Huh7 cells were cultured in RPMI (Gibco 31870) with 10% (v/v) FCS, 0.1 mM nonessential amino acids, 2 mM L-glutamine, and 10 mM HEPES. All cells were kept at 37 °C and 5% (v/v) CO_2.

Primary hepatocytes were obtained by perfusion of mouse liver with collagenase according to published procedures and were kept in Williams E medium (Gibco Nr. A12176-01).

Fatty Acid Labeling. Cultivated mammalian cells were labeled by supplementation of fatty acids in the respective growth media at final concentrations of 5−50 μM. For labeling of mouse liver, the liver was perfused with Williams E medium supplemented with 10 mg mL^{-1} fatty acid free BSA, 66 μM alkyne-oleate, and 33 μM alkyne-palmitate at a flow rate of 5 mL min^{-1}. *E. coli* strain BL 21 were grown in minimal medium (M9 supplemented with 0.5% (w/v) glucose and 3 mg L^{-1} $FeSO_4 \cdot 7H_2O$) and incubated for 3 h with 20 μM alkyne fatty acids in minimal medium plus 5 mg mL^{-1} BSA. *Drosophila melanogaster* L3 larvae were opened by longitudinally cutting the cuticle and incubated in PBS supplemented with 10 mg mL^{-1} BSA and 50 μM alkyne fatty acid for 40 min.

Imaging of TLC Plates. For excitation, we used a LED lamp (10 × 1 W 420 nm LEDs, Roithner Lasertechnik, Vienna, Austria), equipped with a HEBO V01 (Hebo Spezialglas) excitation filter. Images were acquired with a Rolera MGI plus EMCCD camera (Decon Science Tec), equipped with a 494/20 and 572/28 bandpass emission filter

dx.doi.org/10.1021/cb300414v | *ACS Chem. Biol.* 2012, 7, 2004−2011

wheel, all under control of GelPro analyzer (Media Cybernetics) software. Using a macro, at total of 16 images of each plate are taken, with each of the two filters eight images with exposure times between 20 ms and 5 s.

To correct for inhomogeneities in illumination intensity and camera sensitivity, a picture of an empty plate without the emission filter was taken. Using the Fiji software package (www.fiji.sc), fluorescence images were divided through this picture. If necessary, particularly if very small amounts of sample were used, some background bands with broad fluorescence emission can be reduced by subtraction of a picture obtained in the 572 nm (noise) channel from that obtained in the 494 nm (signal) channel. Final quantification was performed using the GelPro analyzer software.

Standard Procedure. All values calculated for 3 cm dishes: Cells are incubated with alkyne-compounds (typically 5−50 μM alkyne fatty acid) in regular growth medium supplemented with 10 mg mL^{-1} fatty acid free BSA and washed twice with 1 mL PBS + 10 mg mL^{-1} fatty acid free BSA and once with 1 mL PBS. Cells are scraped into 0.3 mL PBS and transferred into a 2 mL tube. Methanol (0.6 mL) and chloroform (150 μL) are added, and the tube is briefly vortexed to obtain a single liquid phase with most of the cellular protein forming a precipitate (if a two-phase mixture forms, add methanol dropwise until a single phase forms). The tube is centrifuged at 14000*g* for 2 min, the supernatant is transferred into a fresh tube, and the pellet is discarded (can be used for analysis of protein if necessary). Chloroform (300 μL) and 0.1% (v/v) aqueous acetic acid (600 μL) are added followed by vortexing and centrifugation at 14000*g* for 5 min. The upper aqueous phase is discarded, and the lower organic phase is transferred into a fresh 1.5 mL reaction vessel (Sarstedt Nr. 72.690.001) and dried in a speed-vac. The dry lipid pellet is redissolved by addition of 7 μL chloroform, followed by addition of 30 μL click reaction mixture (5 μL of 44.5 mM 3-azido-7-hydroxycoumarin, 500 μL of 10 mM $[\text{acetonitrile}]_4\text{CuBF}_4$ in acetonitrile, 2 mL ethanol). The tube is incubated in a heating block (Eppendorf Thermomixer comfort, 24 × 1.5 mL block, 42 °C, **no shaking**), until all solvent is condensed under the lid of the tube (typically 3 h). Note that the concentration achieved by evaporation is of crucial importance, because it drives the reaction to completion. The tube is briefly centrifuged, and the lipids are redissolved by mixing for 1 min at 42 °C and applied onto a 20 cm × 20 cm silica TLC plate (no UV-indicator, Merck No. 1.05721.0001). The plate is developed in CHCl_3/MeOH/water/AcOH 65/25/4/1 for 10 cm, dried for 2 min in a warm stream of air, and developed again for 18 cm in hexane/ethyl acetate 1/1. The plate is briefly dried in a stream of warm air and soaked for 5 s in 4% (v/v) *N*,*N*-diisopropylethylamine in hexane. The plate is placed in a hood for 1 min to evaporate excess solvent, followed by fluorescent imaging (ex 420 nm, em 482−502 nm).

For large-scale applications in small dishes, particularly 96-well plates (Supplementary Figure 6), scraping of cells is inefficient and time-consuming. Therefore, lipid extraction is performed on the plate. After labeling and washing, the plate is centrifuged upside down for 1 min at 500*g* to remove excess liquid. Then, CHCl_3/MeOH 1/5 (100 μL per well) is added, and the plate gently agitated for 1 min. This extract is transferred into 1.5 mL tubes, dried in the speed-vac, and click reacted according to the standard protocol. To compensate for the small surface of a 96-well (1/29 of a 6-well), a longer labeling time of 75 min with reduced fatty acid concentrations of 5−20 μM should be selected.

■ ASSOCIATED CONTENT

Supporting Information

Synthetic procedures, supporting information, supplementary figures. This material is available free of charge *via* the Internet at http://pubs.acs.org

■ AUTHOR INFORMATION

Corresponding Author

*E-mail: cthiele@uni-bonn.de.

Notes

The authors declare the following competing financial interest(s): University of Bonn has filed a patent covering the methodology as such and some of the substances described.

■ ACKNOWLEDGMENTS

The authors thankfully acknowledge financial support by the German Federal Ministry for Science and Education (The Virtual Liver, to A.G., K.P., C.P., A.Sh., and C.T.) and the Deutsche Forschungsgemeinschaft (Transregio TRR83 to M.S. and C.T., SFB645 to D.L. and A.St.)

■ ABBREVIATIONS

CE, cholesterol ester; CEPT, CDP-ethanolamine phosphoethanolaminetransferase; CL, cardiolipin; CPT, CDP-choline phosphocholinetransferase; DAG, diacylglycerol; DAGK, diacylglycerol kinase; DGAT, diacylglycerol acyltransferase; FA, fatty acid; G3P, glycerol-3-phosphate; GPAT, glycerophosphate acyltransferase; LPAAT lysophosphatidic acid acyltransferase; MS, mass spectrometry; MS/MS, tandem mass spectrometry; PA, phosphatic acid; PC, phosphatidylcholine; PE phosphatidylethanolamine; PG, phosphatidylglycerol; PI, phosphatidylinositol; PLA2, phospholipase A2; PLC, phospholipase C; PLD, phospholipase D; PS, phosphatidylserine; TAG, triacylglycerol; TLC, thin layer chromatography

■ REFERENCES

(1) Kornberg, A., and Pricer, W. E., Jr. (1953) Enzymatic synthesis of the coenzyme A derivatives of long chain fatty acids. *J. Biol. Chem. 204*, 329−343.

(2) Kolb, H. C., Finn, M. G., and Sharpless, K. B. (2001) Click Chemistry: diverse chemical function from a few good reactions. *Angew. Chem., Int. Ed. 40*, 2004−2021.

(3) Beatty, K. E., Xie, F., Wang, Q., and Tirrell, D. A. (2005) Selective dye-labeling of newly synthesized proteins in bacterial cells. *J. Am. Chem. Soc. 127*, 14150−14151.

(4) Dieterich, D. C., Link, A. J., Graumann, J., Tirrell, D. A., and Schuman, E. M. (2006)) Selective identification of newly synthesized proteins in mammalian cells using bioorthogonal noncanonical amino acid tagging (BONCAT). *Proc. Natl. Acad. Sci. U.S.A. 103*, 9482−9487.

(5) Agard, N. J., Baskin, J. M., Prescher, J. A., Lo, A., and Bertozzi, C. R. (2006) A comparative study of bioorthogonal reactions with azides. *ACS Chem. Biol. 1*, 644−648.

(6) Salic, A., and Mitchison, T. J. (2008) A chemical method for fast and sensitive detection of DNA synthesis in vivo. *Proc. Natl. Acad. Sci. U.S.A. 105*, 2415−2420.

(7) Hannoush, R. N., and Sun, J. (2010) The chemical toolbox for monitoring protein fatty acylation and prenylation. *Nat Chem Biol. 6*, 498−506.

(8) Hang, H. C., Geutjes, E. J., Grotenbreg, G., Pollington, A. M., Bijlmakers, M. J., and Ploegh, H. L. (2007) Chemical probes for the rapid detection of fatty-acylated proteins in mammalian cells. *J. Am. Chem. Soc. 129*, 2744−2745.

(9) Kostiuk, M. A., Corvi, M. M., Keller, B. O., Plummer, G., Prescher, J. A., Hangauer, M. J., Bertozzi, C. R., Rajaiah, G., Falck, J. R., and Berthiaume, L. G. (2008) Identification of palmitoylated mitochondrial proteins using a bio-orthogonal azido-palmitate analogue. *FASEB J. 22*, 721−732.

(10) Martin, B. R., and Cravatt, B. F. (2009) Large-scale profiling of protein palmitoylation in mammalian cells. *Nat. Methods 6*, 135−138.

(11) Milne, S. B., Tallman, K. A., Serwa, R., Rouzer, C. A., Armstrong, M. D., Marnett, L. J., Lukehart, C. M., Porter, N. A., and Brown, H. A. (2010) Capture and release of alkyne-derivatized glycerophospholipids using cobalt chemistry. *Nat. Chem. Biol. 6*, 205−207.

(12) Sivakumar, K., Xie, F., Cash, B. M., Long, S., Barnhill, H. N., and Wang, Q. (2004) A fluorogenic 1,3-dipolar cycloaddition reaction of 3-azidocoumarins and acetylenes. *Org. Lett. 6*, 4603−4606.
(13) Fink, D. W., and Koehler, W. R. (1970) pH effects on fluorescence of umbelliferone. *Anal. Chem. 240*, 990−993.
(14) Laskey, R. A., and Mills, A. D. (1975) Quantitative film detection of ^{3}H and ^{14}C in polyacrylamide gels by fluorography. *Eur. J. Biochem. 56*, 335−341.
(15) Schwudke, D., Oegema, J., Burton, L., Entchev, E., Hannich, J. T., Ejsing, C. S., Kurzchalia, T., and Shevchenko, A. (2006) Lipid profiling by multiple precursor and neutral loss scanning driven by the data-dependent acquisition. *Anal. Chem. 78*, 585−595.
(16) McLaren, D. G., He, T., Wang, S. P., Mendoza, V., Rosa, R., Gagen, K., Bhat, G., Herath, K., Miller, P. L., Stribling, S., Balkovec, J. M., DeVita, R. J., Marsh, D. J., Castro-Perez, J. M., Strack, A., Johns, D. G., Previs, S. F., Hubbard, B. K., and Roddy, T. P. (2011) The use of stable-isotopically labeled oleic acid to interrogate lipid assembly in vivo: assessing pharmacological effects in preclinical species. *J. Lipid. Res. 52*, 1150−1161.
(17) Kuerschner, L., Ejsing, C. S., Ekroos, K., Shevchenko, A., Anderson, K. I., and Thiele, C. (2005) Polyene-lipids: A new tool to image lipids. *Nat. Methods 2*, 39−45.
(18) Yount, J. S., Charron, G., and Hang, H. C. (2012) Bioorthogonal proteomics of 15-hexadecynyloxyacetic acid chemical reporter reveals preferential targeting of fatty acid modified proteins and biosynthetic enzymes. *Bioorg. Med. Chem. 20*, 650−654.
(19) Patel, S. S., and Walt, D. R. (1988) Acetyl coenzyme A synthetase catalyzed reactions of coenzyme A with alpha, beta-unsaturated carboxylic acids. *Anal. Biochem. 170*, 355−360.
(20) Ortiz de Montellano, P. R., and Reich, N. O. (1984) Specific inactivation of hepatic fatty acid hydroxylases by acetylenic fatty acids. *J. Biol. Chem. 259*, 4136−4141.
(21) Muerhoff, A. S., Williams, D. E., Reich, N. O., CaJacob, C. A., Ortiz de Montellano, P. R., and Masters, B. S. (1989) Prostaglandin and fatty acid omega- and (omega-1)-oxidation in rabbit lung. Acetylenic fatty acid mechanism-based inactivators as specific inhibitors. *J. Biol. Chem. 264*, 749−756.
(22) Neef, A. B., and Schultz, C. (2009) Selective fluorescence labeling of lipids in living cells. *Angew. Chem., Int. Ed. 48*, 1498−1500.
(23) Jao, C. Y., Roth, M., Welti, R., and Salic, A. (2009) Metabolic labeling and direct imaging of choline phospholipids in vivo. *Proc. Natl. Acad. Sci. U.S.A. 106*, 15332−15337.
(24) Hannoush, R. N., and Arenas-Ramirez, N. (2009) Imaging the lipidome: omega-alkynyl fatty acids for detection and cellular visualization of lipid-modified proteins. *ACS Chem. Biol. 4*, 581−587.
(25) Raetz, C. R., and Dowhan, W. (1990) Biosynthesis and function of phospholipids in *Escherichia coli*. *J. Biol. Chem. 265*, 1235−1238.
(26) Jones, H. E., Harwood, J. L., Bowen, I. D., and Griffiths, G. (1992) Lipid composition of subcellular membranes from larvae and prepupae of *Drosophila melanogaster*. *Lipids 27*, 984−947.
(27) Kuerschner, L., Richter, D., Hannibal-Bach, H. K., Gaebler, A., Shevchenko, A., Ejsing, C. S., and Thiele, C. (2012) Exogenous ether lipids predominantly target mitochondria. *PLoS One 7*, No. e31342.
(28) Bach, A. C., Ingenbleek, Y., and Frey, A. (1996) The usefulness of dietary medium-chain triglycerides in body weight control: fact or fancy? *J. Lipid Res. 37*, 708−726.
(29) Pegorier, J. P., Duee, P. H., Herbin, C., Laulan, P. Y., Blade, C., Peret, J., and Girard, J. (1988) Fatty acid metabolism in hepatocytes isolated from rats adapted to high-fat diets containing long- or medium-chain triacylglycerols. *Biochem. J. 249*, 801−806.
(30) Mayorek, N., and Bar-Tana, J. (1983) Medium chain fatty acids as specific substrates for diglyceride acyltransferase in cultured hepatocytes. *J. Biol. Chem. 258*, 6789−6792.
(31) Guo, W., Choi, J. K., Kirkland, J. L., Corkey, B. E., and Hamilton, J. A. (2000) Esterification of free fatty acids in adipocytes: a comparison between octanoate and oleate. *Biochem. J. 349*, 463−471.